Rapid Communications

Suppressed energy transport in the strongly disordered Hubbard chain

Maciej Kozarzewski,[1] Marcin Mierzejewski,[2] and Peter Prelovšek[3,4]
[1]*Institute of Physics, University of Silesia, 40-007 Katowice, Poland*
[2]*Department of Theoretical Physics, Faculty of Fundamental Problems of Technology, Wrocław University of Science and Technology, 50-370 Wrocław, Poland*
[3]*J. Stefan Institute, SI-1000 Ljubljana, Slovenia*
[4]*Faculty of Mathematics and Physics, University of Ljubljana, SI-1000 Ljubljana, Slovenia*

(Received 26 April 2019; published 28 June 2019)

We study the dynamics of the energy fluctuations in the Hubbard chain with strong potential disorder that preserves the SU(2) spin symmetry. Within the effective spin-only model that correctly captures relaxation in the situation of localized charges, we show that the decay of local energy correlations is suppressed and is at least marginally nonergodic, being qualitatively different from the subdiffusive dynamics and relaxation of local spins. The anomalous behavior can be traced back to the singular distribution of effective exchange couplings. Numerical results for the dynamical thermal conductivity within the full Hubbard model confirm that the energy (thermal) transport is closer to the charge dynamics, which appears to be also marginally localized in a wide parameter range.

DOI: 10.1103/PhysRevB.99.241113

Introduction. The dynamics of strongly disordered many-body systems has recently attracted significant attention. The main interest focused on the phenomenon of many–body localization (MBL) [1,2] which has been supported by a vast amount of numerical investigations, predominantly of disordered one-dimensional (1D) model of interacting spinless fermions or equivalent XXZ spin chains with random magnetic field. In particular, it has been recognized that such MBL systems exhibit several unique properties: logarithmic growth of the entanglement entropy [3–8], absence of thermalization [7–27], vanishing steady transport, [28–35] and suppressed heating effects in driven systems [34,36–41]. It has also been shown that these properties originate from the presence of local integrals of motion [10,21,22,42–47]. While the above evidence of MBL holds for systems, where the disorder breaks the SU(2) symmetry, the situation is far more complex if the latter symmetry is preserved despite the presence of the disorder [48–54]. It is the case for the 1D Hubbard chain with spin-1/2 fermions where disorder enters only via the charge potential. Such model is directly relevant also for the experiments on cold-fermion lattices [12,55–57]. Then, the localization may occur only in the charge subsystem [47,52,58,59,59] (partial MBL) unless one introduces an additional mechanism that breaks the SU(2) symmetry [47,60,61]. On the other hand, the delocalized spins in the SU(2) invariant case exhibit anomalous subdiffusive transport [52,62].

While the theoretical as well as experimental investigation of the disordered Hubbard chain focused on the charge (density) and spin dynamics, the relevant question on the character of energy (thermal) transport, responsible for the system thermalization, has not been addressed. In the following we show that the spatial energy fluctuations are, in analogy with charge, almost localized and decay not faster than $\log(t)$. At the same time, the spatial spin fluctuations undergo the subdiffusive relaxation, $\sim t^{\alpha}$ with $\alpha > 0$ being large enough to clearly distinguish between the power-law and the logarithmic dependencies. We numerically show and also qualitatively explain this result within an effective spin-only model [62], where the charge localization is introduced as an assumption. However, we confirm the suppression of the energy (thermal) transport also via the direct numerical studies of the dynamical energy (thermal) conductivity within the full 1D disordered Hubbard chain. This property appears to be consistent with the novel nonergodic phases recently reported in Refs. [54] and partially also in [63].

Disordered Hubbard chain and the effective spin model. We study dynamics and transport properties of the disordered Hubbard chain,

$$H = -t_{\rm h}\sum_{i\sigma}(c^{\dagger}_{i+1\sigma}c_{i\sigma} + {\rm H.c.}) + \sum_i \varepsilon_i n_i + U\sum_i \left(n_{i\uparrow} - \frac{1}{2}\right)\left(n_{i\downarrow} - \frac{1}{2}\right), \quad (1)$$

where $c^{\dagger}_{i+1\sigma}$ creates a fermion with spin $\sigma = \pm\frac{1}{2}$, $n_i = n_{i\uparrow} + n_{i\downarrow}$, and $n_{i\sigma} = c^{\dagger}_{i\sigma}c_{i\sigma}$. The chain consists of L sites and N electrons, where we fix the total spin projection $S^z_{\rm tot} = 0$ and set the hopping integral $t_h = 1$. The charge potential is chosen as a random variable with a uniform distribution, $\varepsilon_i \in [-W, W]$. In the present work we focus on the energy (thermal) dynamics and transport, comparing it with subdiffusive spin dynamics as established previously in Ref. [62]. In analogy to Refs. [52,62], we first assume that charge is frozen and the energy dynamics is possible only via delocalized spin fluctuations within the effective spin-only model. The stronger the disorder is, the more justified is this simplification. Later on, we relax this assumption and discuss numerical results also for the full Hubbard model.

Let us first consider the effective spin model. We recall the main steps of its derivation and refer to Ref. [62] for more details. We use the single-particle eigenstates of the noninteracting model (Anderson states), $|a\rangle$, as the single-particle basis. These states are sorted according to the maxima of the corresponding wave functions, $|\langle i|a\rangle|$, in such a way that the Anderson states $|a\rangle$ and $|a+1\rangle$ are the nearest neighbors in the real space. Then, we rewrite the Coulomb repulsion U in Eq. (1) in the latter basis and neglect terms which alter the occupations of the Anderson states, i.e., we assume $n_{a\uparrow} + n_{a\downarrow} = \text{const}$. The remaining terms become the effective spin model [62],

$$H = -2U \sum_a \tilde{J}_a \vec{S}_a \cdot \vec{S}_{a+1} = \sum_a h_a, \tag{2}$$

where h_a is the energy density operator and the summation is carried out only over singly occupied Anderson states. The number of such states equals $\tilde{N} \simeq N - N^2/(2L)$ and $\tilde{N}$ is the effective length of the spin chain which determines the complexity of numerical calculations. Here, we use standard spin operators $S^z_a = \frac{1}{2}(n_{a\uparrow} - n_{a\downarrow})$, $S^+_a = c^\dagger_{a\uparrow} c_{a\downarrow}$, $S^-_a = c^\dagger_{a\downarrow} c_{a\uparrow}$, where $c^\dagger_{a\sigma}$ denotes the fermionic creation operator in the Anderson state $|a\rangle$ and with spin $\sigma = \pm 1/2$. We note that the effective exchange interaction is ferromagnetic, $-2U\tilde{J}_a < 0$, where $0 \leqslant \tilde{J}_a \leqslant 1$ has been shown [62] to be a random variable with the probability distribution,

$$f_{\tilde{J}}(\tilde{J}) = \tilde{\lambda}\tilde{J}^{\tilde{\lambda}-1}, \quad \tilde{\lambda} = \lambda/d. \tag{3}$$

Here, λ is the Anderson localization length within the noninteracting system, i.e., for the Hamiltonian (1) with $U = 0$, and d is the average real-space distance between singly occupied Anderson states $d = L/\tilde{N}$. For strong disorder $\lambda < d$ and the distribution function is singular at $\tilde{J} = 0$, whereby the latter singularity has been shown to be responsible for the anomalous (subdiffusive) spin dynamics and transport in the disordered Hubbard model [62]. The very same model, Eqs. (2) and (3), has been recently studied also in Ref. [54] for its nonergodic dynamics.

Results within the effective model. We discuss relaxation of spatial fluctuations for spin and energy density. For this sake, we calculate correlation functions

$$C^S(t) = \left\langle \frac{\langle S^z_a(t) S^z_a\rangle - \langle S^z_a\rangle^2}{\langle S^z_a S^z_a\rangle - \langle S^z_a\rangle^2} \right\rangle_{dis,a}, \tag{4}$$

$$C^h(t) = \left\langle \frac{\langle h_a(t) h_a\rangle - \langle h_a\rangle^2}{\langle h_a h_a\rangle - \langle h_a\rangle^2} \right\rangle_{dis,a}, \tag{5}$$

where $\langle \cdots \rangle = \mathrm{Tr}(\cdots)/\mathrm{Tr}(1)$ denotes averaging over infinite-temperature canonical ensemble. $\langle \cdots \rangle_{dis,a}$ denotes averaging over $\tilde{N}$ Anderson states (i.e., positions in the real space) and $N_s > 1$ realizations of disorder. Both functions are by definition normalized so that $C^{S,h}(t=0) = 1$. We focus here on the asymptotic time dependencies, $t \gg 1$, of both correlation functions. We use two complementary numerical methods to verify the consistency of results. Namely, for $\tilde{N} \sim 18$ and times $t \lessapprox 10^3$ we use a time-dependent Lanczos method [64], whereas arbitrary long times but smaller systems $\tilde{L} \leqslant 14$ are studied via the exact diagonalization (ED). Within the ED method, the averaging $\langle \cdots \rangle$ is carried out over all eigenstates

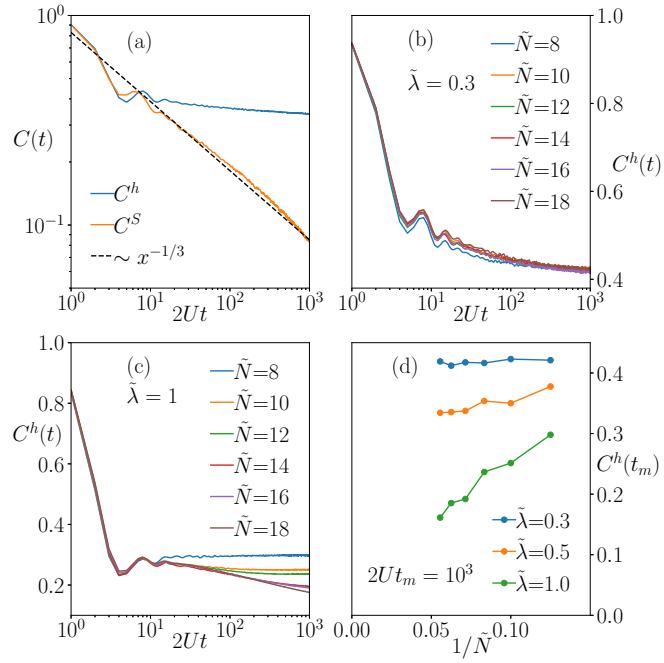

FIG. 1. Results from the Lanczos propagation method averaged over $N_s = 2000$ realizations of disorder. (a) Spin density $C^S(t)$ and energy density $C^h(t)$ correlation functions for $\tilde{\lambda} = 0.5$ and $\tilde{N} = 18$. Dashed line shows analytical prediction for asymptotic dynamics, $C^S(t) \sim t^{-\tilde{\lambda}/(1+\tilde{\lambda})}$. (b) and (c) $C^h(t)$ for $\tilde{\lambda} = 0.3$ and $\tilde{\lambda} = 1.0$, respectively. (d) Finite-size scaling of $C^h(t_m)$ for the longest accessible time, $2Ut_m = 10^3$.

of Hamiltonian when $\langle S^z_a\rangle = \langle h_a\rangle = 0$. However, for the Lanczos method, it is replaced by the averaging over a few random initial wave functions. These approaches give quantitatively consistent results for system sizes which are accessible to both methods.

Figure 1(a) shows numerical results of the Lanczos time propagation for $C^S(t)$ and $C^h(t)$, together with the analytical prediction for asymptotic dependence, $C^S(t \gg 1) \sim t^{-\tilde{\lambda}/(1+\tilde{\lambda})}$, derived in Ref. [62] within the weak-link (Griffiths) scenario [30,57,65,66]. While $C^S(t)$ indeed decays subdiffusively, the relaxation of $C^h(t)$ is significantly suppressed. In fact, it is quite delicate to establish whether the energy stiffness $C^h_0 = C^h(t \to \infty)$ eventually remains finite or decays to zero. To clarify this question, we plot in Figs. 1(b) and 1(c) $C^h(t)$ for various $\tilde{N}$, but for two different disorders which correspond to $\tilde{\lambda} = 0.3$ and $\tilde{\lambda} = 1.0$, respectively. Here, $\tilde{\lambda} = 0.3$ leads via Eq. (3) to a singular distribution of $\tilde{J}$. It is evident that in this case the stiffness $C^h_0 > 0$ is not a finite-size effect and its nonzero value is essentially $\tilde{N}$ independent. On the other hand, results in Fig. 1(c) for $\tilde{\lambda} = 1$, which correspond to a uniform (nonsingular) distribution of $\tilde{J}$, reveal evident finite-size dependence. This indicates that in the thermodynamic limit, $\tilde{N} \to \infty$, we are dealing with an ergodic behavior and vanishing energy stiffness $C^h_0 = 0$. In order to get a further insight into the finite-size effects, we plot in Fig. 1(d) $C^h(t_m)$ obtained for the longest accessible times $2Ut_m = 10^3$ vs $1/\tilde{N}$ for different $\tilde{\lambda}$. Again, $C^h(t_m)$ vs $1/\tilde{N}$ clearly decays to zero for a nonsingular distribution of J ($\tilde{\lambda} = 1$), while results for smaller $\tilde{\lambda} \leqslant 0.5$ are more consistent with finite $C^h_0 > 0$ and

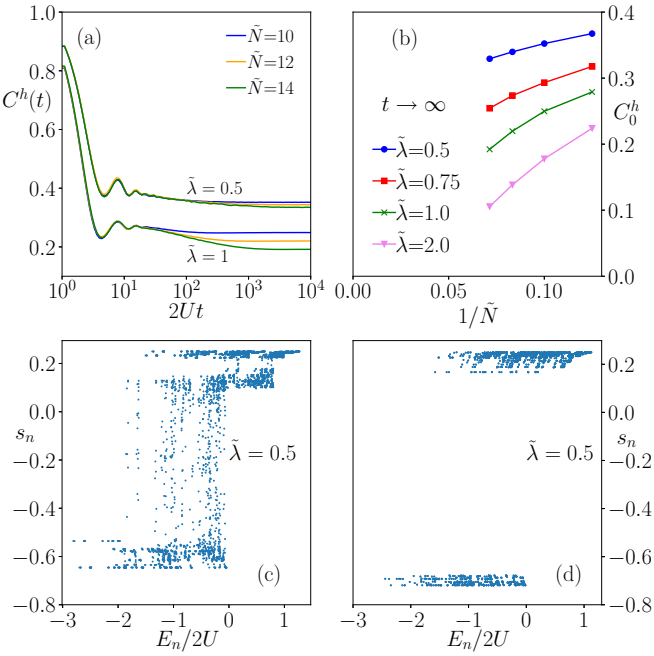

FIG. 2. Results from the ED method averaged over $N_s \gtrapprox 10^4$ realizations of disorder. (a) The same as in Fig. 1(c) for $\tilde{\lambda}=0.5$ and $\tilde{\lambda}=1$ but for longer times. (b) Finite-size scaling of the energy stiffness C_0^h vs $1/\tilde{N}$. (c) and (d) Diagonal matrix elements, $s_n=\langle n|\vec{S}_a\cdot\vec{S}_{a+1}|n\rangle$ vs eigenenergy E_n obtained for a bond with the largest J_a for $\tilde{N}=14$ and two particular realizations of disorder corresponding to the same $\tilde{\lambda}=0.5$.

the localization of the energy fluctuations. Still, it should be acknowledged that data in Fig. 1(d) are obtained for long but finite time and are still scattered due to sample-to-sample fluctuations, and therefore it is difficult to carry out a clear-cut finite-size scaling.

In order to investigate further the energy stiffness C_0^h, we have carried out also ED calculations which, in principle, allow one to reach arbitrarily long times $t\to\infty$, relating C_0^h to the diagonal matrix elements within the eigenfunction basis. Results have been averaged over $N_s=10^5, 3\times10^4$ and 10^4 realizations of disorder for $\tilde{N}=10, 12, 14$, respectively. Figure 2(a) confirms for both presented $\tilde{\lambda}=0.5$ and 1 that $C^h(t)$ shows very slow logarithmic decay and eventually saturates for $t>t_s$. However, t_s increases with the system size, hence the saturation might be a finite-size effect. In order to test the latter possibility, we have carried out the finite-size analysis of the stiffness C_0^h, shown in Fig. 2(b). The negative curvature of C_0^h vs $1/\tilde{N}$ suggests that in the limit $\tilde{N}\to\infty$ we may even have $C_0^h=0$ for arbitrary $\tilde{\lambda}>0$. While this is quite clear for $\tilde{\lambda}\sim1$, in order to observe complete relaxation of $C_0^h\to0$ for $\tilde{\lambda}\ll1$ one needs extremely large system sizes which are far beyond the limitations of our numerical methods. This observation is fully consistent with conclusions in Ref. [54].

At first sight, it is quite surprising that spin and energy dynamics (i.e., subdiffusive vs nonergodic, respectively) are qualitatively different at strong disorder. In order to explain this difference in relaxations we study the diagonal matrix elements of operators which enter the energy density, i.e., $s_{n,a}=\langle n|\vec{S}_a\cdot\vec{S}_{a+1}|n\rangle$. Similar quantity has recently been studied in Ref. [54]. For a nondegenerate energy spectrum, analogous matrix elements for local spin $\langle n|S_a^z|n\rangle=0$ vanish due to spin-rotation SU(2) symmetry, hence $C^S(t\to\infty)=0$ precluding finite local spin stiffness and the spin localization. However, the latter argument does not apply to energy fluctuations. Figures 2(c) and 2(d) show typical structures of $s_{n,a}$ vs eigenenergies E_n, obtained for the links with the largest exchange interactions $\tilde{J}_a$ and for two different disorder configurations corresponding to the same $\tilde{\lambda}=0.5$. One may observe that in both realizations in Figs. 2(c) and 2(d) $s_{n,a}$ is essentially fluctuating between two values, either close to $-3/4$ (spin singlet) or $1/4$ (spin triplet), which both just represent the limiting values and are both blocking locally the energy transport. It explains the saturation of $C^h(t\to\infty)$, and consequently $C_0^h>0$, at least for finite systems.

Conductivities within full Hubbard model. The effective model has been derived under the assumption that charge degrees of freedom are frozen. While such an assumption is better justified for the studies of spin dynamics (which is relatively fast), the results and conclusions on the energy fluctuations and the energy (thermal) transport should be tested also for the full starting Hubbard model, Eq. (1). For this sake we study numerically dynamical transport response functions within the half-filled ($N=L$) Hubbard model, as relevant at high temperature ($\beta=1/T\to0$). In the latter limit, the linear-response charge, spin, and thermal (energy) dynamical conductivities are given, respectively, by $\sigma^{c,S}(\omega)=\beta\tilde{\sigma}^{c,S}(\omega)$ and $\kappa(\omega)=\beta^2\tilde{\sigma}^t(\omega)$, where

$$\tilde{\sigma}^{c,S,t}(\omega)=\frac{1}{L}\mathrm{Re}\int_0^\infty dt\, e^{i\omega t}\langle I_{c,S,t}(t)I_{c,S,t}\rangle, \tag{6}$$

are dynamical quantities actually calculated and remaining finite even in the limit $\beta\to0$. Here, the corresponding current operators following from the model (1) are given by

$$I_c=\sum_{j,\sigma}\mathcal{I}_{j\sigma},\quad I_S=\sum_{j,\sigma}\sigma\mathcal{I}_{j\sigma}, \tag{7}$$

$$I_t=-\sum_{j,\sigma}(ic^\dagger_{j+1\sigma}c_{j-1\sigma}+\mathrm{H.c.}) + \sum_{j,\sigma}\mathcal{I}_{j\sigma}\left(\frac{\varepsilon_j+\varepsilon_{j+1}}{2}+U\frac{n_{l\bar{\sigma}}+n_{l+1\bar{\sigma}}-1}{2}\right), \tag{8}$$

and $\mathcal{I}_{j\sigma}=i(c^\dagger_{j+1\sigma}c_{j,\sigma}-c^\dagger_{j\sigma}c_{j+1\sigma})$.

For the numerical calculations of $\tilde{\sigma}^{c,S,t}(\omega)$ we employ the microcanonical Lanczos method (MCLM) [67,68] on the Hubbard chains of maximum length $L=14$. The high-frequency resolution is achieved by a large number of Lanczos steps, $N_L=3000$, allowing for $\delta\omega\propto L/N_L\sim0.003$, while the sample averaging is performed over $N_s\sim30$–100 disorder realizations. In Fig. 3 we present some characteristic results for dynamical conductivities, $\bar{\sigma}^{c,S,t}(\omega)$, for more transparent comparison normalized by their sum rules, i.e., $\bar{\sigma}(\omega)=\tilde{\sigma}(\omega)/\int d\omega'\tilde{\sigma}(\omega')$.

First, in Figs. 3(a) and 3(b) we present the comparison of results for $\bar{\sigma}^S(\omega)$ and $\bar{\sigma}^t(\omega)$, as obtained for different sizes $L=10, 12, 14$. Apart from the high-ω regime, where spectra are strongly sample dependent and need substantial sample averaging, $N_s\gg1$, low-ω regime is very reproducible

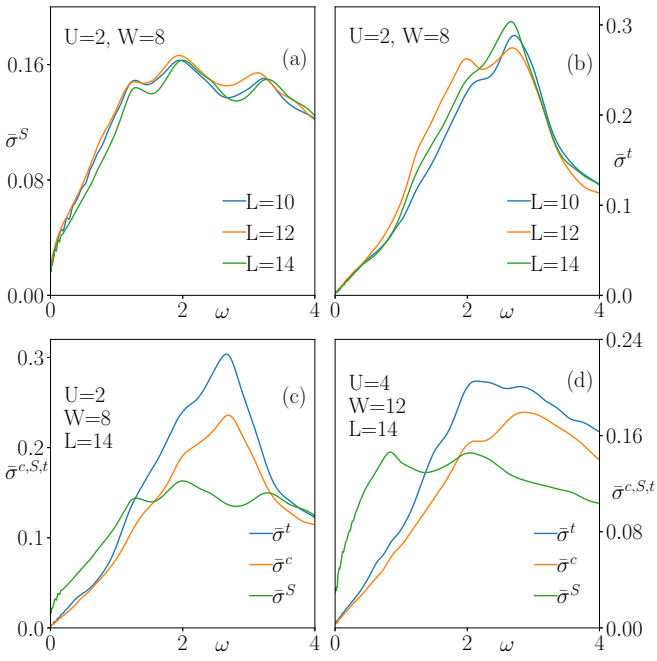

FIG. 3. Normalized charge, spin, and thermal dynamical conductivities, as obtained via the numerical MCLM in different Hubbard chains with large disorder. (a) and (b) show the finite-size effects (comparison of results for $L = 10$–14 systems, of $\bar{\sigma}^S(\omega)$ and $\bar{\sigma}^t(\omega)$, respectively, for fixed disorder $W = 8$ and $U = 2$. (c) and (d) show the comparison of $\bar{\sigma}^{c,S,t}(\omega)$ for two different parameter sets, obtained for the largest $L = 14$.

even at modest N_s and quite L independent. Results for $\bar{\sigma}^{c,S,t}(\omega)$, obtained at largest $L = 14$, are then presented in Figs. 3(c) and 3(d) for two different sets of parameters, $U = 2, W = 8$ and $U = 4, W = 12$, both corresponding to large disorder. The qualitative difference between considered dynamical conductivities at low $\omega \ll 1$ is evident. While the spin transport follows the subdiffusive behavior, $\bar{\sigma}^S(\omega) \propto \omega^\alpha$ with $\alpha < 1$, the charge as well as the energy follow nearly linear variation $\bar{\sigma}^c(\omega) \propto \omega^\gamma$, $\bar{\sigma}^t(\omega) \propto \omega^\delta$ with $\gamma \sim \delta \sim 1$. We note that $\delta \sim 1$ is just the marginal MBL case which is consistent with the $\log(t)$ decay of the local energy correlation function, $C^h(t)$, found previously in the effective spin model. We have carried out calculations (not shown) also for stronger disorder $W = 16, 20$ and for interactions $U = 2, 4$. In the low-frequency regime, $\omega \lesssim 0.5$, all the dynamical conductivities are qualitatively very similar to the results shown in Fig. 3. In particular, we have found $\alpha < 1$ and $\gamma \sim 1$ for all the considered cases. While the spin dynamics becomes slower for stronger disorder, we have not found any signature of spin localization. Moreover, we should also stress the observation that we obtain the charge exponent $\gamma \sim 1$ instead of $\gamma > 1$ required for localization, i.e., the charge appears to be only marginally localized.

Conclusions. It is by now well established for the 1D Hubbard model with (charge) potential disorder that there cannot be the regime of full MBL. This result originates from the remaining SU(2) spin symmetry and leads to qualitatively different dynamics of charge and spin degrees of freedom, well documented in the previous works [52,54,62] as well as in the present study. It follows from the present investigations that the thermal (energy) transport responsible for the thermal equilibration, qualitatively follows that of the charge (particle density). Namely, the spatial energy fluctuations $C^h(t)$ as calculated within the effective spin model relax nearly logarithmically in time and for large disorder, e.g., effective $\tilde{\lambda} < 0.5$, seem to result in a saturation and a finite local energy stiffness $C^h_0 > 0$. However, we cannot exclude the possibility that in very large system $L \to \infty$ and after extremely long evolution, the energy equilibrates, i.e., $C^h(t \to \infty) \to 0$, which is still in sharp contrast with the relatively fast relaxation of $C^S(t)$. The origin of qualitative different spin and energy dynamics can be understood in the framework of the effective spin model, as emerging from three spin processes involved in the energy spread being essentially blocked due to singular distribution of the effective exchange interaction $\tilde{J}_a$. The numerical study of the full Hubbard model confirms that the low-ω dynamical thermal conductivity $\bar{\sigma}^t(\omega) \propto \omega^\delta$, $\delta \sim 1$ indicates on the marginally localized energy fluctuations. We have also found that qualitatively $\bar{\sigma}^t(\omega) \propto \bar{\sigma}^c(\omega)$, i.e., the spin contribution to the energy transport is as well suppressed as in the effective spin model. In contrast to the latter model, the results presented for the Hubbard model indicate that $\bar{\sigma}^c(\omega) \propto \omega^\delta$, $\delta \sim 1$, meaning that the charge remains only marginally localized and nonergodic, even at largest disorders. This might soften some conclusion on the strict charge localization in numerical and experimental studies; still the effect can be distinguished only at extremely long times and very large systems.

Acknowledgments. This work is supported by the National Science Centre, Poland via project 2016/23/B/ST3/00647 (M.M. and M.K.). P.P. acknowledges the support by the program P1-0044 of the Slovenian Research Agency.

[1] D. M. Basko, I. L. Aleiner, and B. L. Altshuler, Metal–insulator transition in a weakly interacting many-electron system with localized single-particle states, Ann. Phys. NY) **321**, 1126 (2006).

[2] V. Oganesyan and D. A. Huse, Localization of interacting fermions at high temperature, Phys. Rev. B **75**, 155111 (2007).

[3] M. Žnidarič, T. Prosen, and P. Prelovšek, Many-body localization in the Heisenberg XXZ magnet in a random field, Phys. Rev. B **77**, 064426 (2008).

[4] J. H. Bardarson, F. Pollmann, and J. E. Moore, Unbounded Growth of Entanglement in Models of Many-Body Localization, Phys. Rev. Lett. **109**, 017202 (2012).

[5] J. A. Kjäll, J. H. Bardarson, and F. Pollmann, Many-Body Localization in a Disordered Quantum Ising Chain, Phys. Rev. Lett. **113**, 107204 (2014).

[6] M. Serbyn, Z. Papić, and D. A. Abanin, Universal Slow Growth of Entanglement in Interacting Strongly Disordered Systems, Phys. Rev. Lett. **110**, 260601 (2013).

[7] M. Serbyn, Z. Papić, and D. A. Abanin, Criterion for Many-Body Localization-Delocalization Phase Transition, Phys. Rev. X **5**, 041047 (2015).

[8] D. J. Luitz, N. Laflorencie, and F. Alet, Extended slow dynamical regime prefiguring the many-body localization transition, Phys. Rev. B **93**, 060201(R) (2016).

[9] A. Pal and D. A. Huse, Many-body localization phase transition, Phys. Rev. B **82**, 174411 (2010).

[10] M. Serbyn, Z. Papić, and D. A. Abanin, Local Conservation Laws and the Structure of the Many-Body Localized States, Phys. Rev. Lett. **111**, 127201 (2013).

[11] Y. Bar Lev and D. R. Reichman, Dynamics of many-body localization, Phys. Rev. B **89**, 220201(R) (2014).

[12] M. Schreiber, S. S. Hodgman, P. Bordia, H. P. Lüschen, M. H. Fischer, R. Vosk, E. Altman, U. Schneider, and I. Bloch, Observation of many-body localization of interacting fermions in a quasi-random optical lattice, Science **349**, 842 (2015).

[13] V. Khemani, R. Nandkishore, and S. L. Sondhi, Nonlocal adiabatic response of a localized system to local manipulations, Nat. Phys. **11**, 560 (2015).

[14] I. V. Gornyi, A. D. Mirlin, and D. G. Polyakov, Interacting Electrons in Disordered Wires: Anderson Localization and Low-*t* Transport, Phys. Rev. Lett. **95**, 206603 (2005).

[15] E. Altman and R. Vosk, Universal dynamics and renormalization in many-body-localized systems, Annu. Rev. Condens. Matter Phys. **6**, 383 (2015).

[16] A. De Luca and A. Scardicchio, Ergodicity breaking in a model showing many-body localization, Europhys. Lett. **101**, 37003 (2013).

[17] C. Gramsch and M. Rigol, Quenches in a quasidisordered integrable lattice system: Dynamics and statistical description of observables after relaxation, Phys. Rev. A **86**, 053615 (2012).

[18] A. De Luca, B. L. Altshuler, V. E. Kravtsov, and A. Scardicchio, Anderson Localization on the Bethe Lattice: Nonergodicity of Extended States, Phys. Rev. Lett. **113**, 046806 (2014).

[19] D. A. Huse, R. Nandkishore, V. Oganesyan, A. Pal, and S. L. Sondhi, Localization-protected quantum order, Phys. Rev. B **88**, 014206 (2013).

[20] R. Nandkishore and D. A. Huse, Many-body-localization and thermalization in quantum statistical mechanics, Annu. Rev. Condens. Matter Phys. **6**, 15 (2015).

[21] L. Rademaker and M. Ortuño, Explicit Local Integrals of Motion for the Many-Body Localized State, Phys. Rev. Lett. **116**, 010404 (2016).

[22] A. Chandran, I. H. Kim, G. Vidal, and D. A. Abanin, Constructing local integrals of motion in the many-body localized phase, Phys. Rev. B **91**, 085425 (2015).

[23] V. Ros, M. Müller, and A. Scardicchio, Integrals of motion in the many-body localized phase, Nucl. Phys. B **891**, 420 (2015).

[24] J. Eisert, M. Friesdorf, and C. Gogolin, Quantum many-body systems out of equilibrium, Nat. Phys. **11**, 124 (2015).

[25] M. Serbyn, M. Knap, S. Gopalakrishnan, Z. Papić, N. Y. Yao, C. R. Laumann, D. A. Abanin, M. D. Lukin, and E. A. Demler, Interferometric Probes of Many-Body Localization, Phys. Rev. Lett. **113**, 147204 (2014).

[26] P. Sierant, D. Delande, and J. Zakrzewski, Many-body localization due to random interactions, Phys. Rev. A **95**, 021601(R) (2017).

[27] P. Prelovšek, O. S. Barišić, and M. Mierzejewski, Reduced-basis approach to many-body localization, Phys. Rev. B **97**, 035104 (2018).

[28] T. C. Berkelbach and D. R. Reichman, Conductivity of disordered quantum lattice models at infinite temperature: Many-body localization, Phys. Rev. B **81**, 224429 (2010).

[29] O. S. Barišić and P. Prelovšek, Conductivity in a disordered one-dimensional system of interacting fermions, Phys. Rev. B **82**, 161106(R) (2010).

[30] K. Agarwal, S. Gopalakrishnan, M. Knap, M. Müller, and E. Demler, Anomalous Diffusion and Griffiths Effects Near the Many-Body Localization Transition, Phys. Rev. Lett. **114**, 160401 (2015).

[31] Y. Bar Lev, G. Cohen, and D. R. Reichman, Absence of Diffusion in an Interacting System of Spinless Fermions on a One-Dimensional Disordered Lattice, Phys. Rev. Lett. **114**, 100601 (2015).

[32] R. Steinigeweg, J. Herbrych, F. Pollmann, and W. Brenig, Scaling of the optical conductivity in the transition from thermal to many-body localized phases, Phys. Rev. B **94**, 180401(R) (2016).

[33] O. S. Barišić, J. Kokalj, I. Balog, and P. Prelovšek, Dynamical conductivity and its fluctuations along the crossover to many-body localization, Phys. Rev. B **94**, 045126 (2016).

[34] M. Kozarzewski, P. Prelovšek, and M. Mierzejewski, Distinctive response of many-body localized systems to a strong electric field, Phys. Rev. B **93**, 235151 (2016).

[35] P. Prelovšek and J. Herbrych, Self-consistent approach to many-body localization and subdiffusion, Phys. Rev. B **96**, 035130 (2017).

[36] D. A. Abanin, W. De Roeck, W. W. Ho, and F. Huveneers, Effective Hamiltonians, prethermalization, and slow energy absorption in periodically driven many-body systems, Phys. Rev. B **95**, 014112 (2017).

[37] D. A. Abanin, W. De Roeck, and F. Huveneers, Exponentially Slow Heating in Periodically Driven Many-Body Systems, Phys. Rev. Lett. **115**, 256803 (2015).

[38] P. Ponte, Z. Papić, F. Huveneers, and D. A. Abanin, Many-Body Localization in Periodically Driven Systems, Phys. Rev. Lett. **114**, 140401 (2015).

[39] P. Bordia, H. Lüschen, U. Schneider, M. Knap, and I. Bloch, Periodically driving a many-body localized quantum system, Nat. Phys. **13**, 460 (2017).

[40] S. Choi, J. Choi, R. Landig, G. Kucsko, H. Zhou, J. Isoya, F. Jelezko, S. Onoda, H. Sumiya, V. Khemani, C. von Keyserlingk, N. Y. Yao, E. Demler, and M. D. Lukin, Observation of discrete time-crystalline order in a disordered dipolar many-body system, Nature (London) **543**, 221 (2017).

[41] J. Zhang, P. W. Hess, A. Kyprianidis, P. Becker, A. Lee, J. Smith, G. Pagano, I.-D. Potirniche, A. C. Potter, A. Vishwanath, N. Y. Yao, and C. Monroe, Observation of a discrete time crystal, Nature (London) **543**, 217 (2017).

[42] D. A. Huse, R. Nandkishore, and V. Oganesyan, Phenomenology of fully many-body-localized systems, Phys. Rev. B **90**, 174202 (2014).

[43] J. Z. Imbrie, V. Ros, and A. Scardicchio, Local integrals of motion in many–body localized systems, Ann. Phys. (NY) **529**, 1600278 (2017).

[44] T. E. O'Brien, D. A. Abanin, G. Vidal, and Z. Papić, Explicit construction of local conserved operators in disordered many-body systems, Phys. Rev. B **94**, 144208 (2016).

[45] S. Inglis and L. Pollet, Accessing Many-Body Localized States through the Generalized Gibbs Ensemble, Phys. Rev. Lett. **117**, 120402 (2016).

[46] M. Goihl, M. Gluza, C. Krumnow, and J. Eisert, Construction of exact constants of motion and effective models for many-body localized systems, Phys. Rev. B **97**, 134202 (2018).

[47] M. Mierzejewski, M. Kozarzewski, and P. Prelovšek, Counting local integrals of motion in disordered spinless-fermion and Hubbard chains, Phys. Rev. B **97**, 064204 (2018).

[48] A. C. Potter and R. Vasseur, Symmetry constraints on many-body localization, Phys. Rev. B **94**, 224206 (2016).

[49] A. Chandran, V. Khemani, C. R. Laumann, and S. L. Sondhi, Many-body localization and symmetry-protected topological order, Phys. Rev. B **89**, 144201 (2014).

[50] I. V. Protopopov, W. W. Ho, and D. A. Abanin, Effect of SU(2) symmetry on many-body localization and thermalization, Phys. Rev. B **96**, 041122(R) (2017).

[51] A. J. Friedman, R. Vasseur, A. C. Potter, and S. A. Parameswaran, Localization-protected order in spin chains with non-Abelian discrete symmetries, Phys. Rev. B **98**, 064203 (2018).

[52] P. Prelovšek, O. S. Barišić, and M. Žnidarič, Absence of full many-body localization in the disordered Hubbard chain, Phys. Rev. B **94**, 241104(R) (2016).

[53] S. A. Parameswaran and S. Gopalakrishnan, Spin-catalyzed hopping conductivity in disordered strongly interacting quantum wires, Phys. Rev. B **95**, 024201 (2017).

[54] I. V. Protopopov, R. K. Panda, T. Parolini, A. Scardicchio, E. Demler, and D. A. Abanin, Non-Abelian symmetries and disorder: A broad non-ergodic regime and anomalous thermalization, arXiv:1902.09236.

[55] J.-Y. Choi, S. Hild, J. Zeiher, P. Schauß, A. Rubio-Abadal, T. Yefsah, V. Khemani, D. A. Huse, I. Bloch, and C. Gross, Exploring the many-body localization transition in two dimensions, Science **352**, 1547 (2016).

[56] P. Bordia, H. P. Lüschen, S. S. Hodgman, M. Schreiber, I. Bloch, and U. Schneider, Coupling Identical 1D Many-Body Localized Systems, Phys. Rev. Lett. **116**, 140401 (2016).

[57] P. Bordia, H. Lüschen, S. Scherg, S. Gopalakrishnan, M. Knap, U. Schneider, and I. Bloch, Probing Slow Relaxation and Many-Body Localization in Two-Dimensional Quasiperiodic Systems, Phys. Rev. X **7**, 041047 (2017).

[58] R. Mondaini and M. Rigol, Many-body localization and thermalization in disordered Hubbard chains, Phys. Rev. A **92**, 041601(R) (2015).

[59] J. Bonča and M. Mierzejewski, Delocalized carriers in the t-J model with strong charge disorder, Phys. Rev. B **95**, 214201 (2017).

[60] G. Lemut, M. Mierzejewski, and J. Bonča, Complete Many-Body Localization in the t-J Model Caused by a Random Magnetic Field, Phys. Rev. Lett. **119**, 246601 (2017).

[61] M. Środa, P. Prelovšek, and M. Mierzejewski, Instability of subdiffusive spin dynamics in strongly disordered Hubbard chain, Phys. Rev. B **99**, 121110(R) (2019).

[62] M. Kozarzewski, P. Prelovšek, and M. Mierzejewski, Spin Subdiffusion in the Disordered Hubbard Chain, Phys. Rev. Lett. **120**, 246602 (2018).

[63] M. Schecter, T. Iadecola, and S. Das Sarma, Configuration-controlled many-body localization and the mobility emulsion, Phys. Rev. B **98**, 174201 (2018).

[64] T. J. Park and J. C. Light, Unitary quantum time evolution by iterative Lanczos reduction, J. Chem. Phys. **85**, 5870 (1986).

[65] K. Agarwal, E. Altman, E. Demler, S. Gopalakrishnan, D. A. Huse, and M. Knap, Rare region effects and dynamics near the many body localization transition, Ann. Phys. (NY) **529**, 1600326 (2017).

[66] H. P. Lüschen, P. Bordia, S. Scherg, F. Alet, E. Altman, U. Schneider, and I. Bloch, Observation of Slow Dynamics near the Many-Body Localization Transition in One-Dimensional Quasiperiodic Systems, Phys. Rev. Lett. **119**, 260401 (2017).

[67] M. W. Long, P. Prelovšek, S. El Shawish, J. Karadamoglou, and X. Zotos, Finite-temperature dynamical correlations using the microcanonical ensemble and the Lanczos algorithm, Phys. Rev. B **68**, 235106 (2003).

[68] P. Prelovšek and J. Bonča, Ground state and finite temperature Lanczos methods, *Strongly Correlated Systems—Numerical Methods* (Springer, Berlin, 2013).